Acta Neuropathol (2006) 111: 168–177
DOI 10.1007/s00401-005-0024-x

ORIGINAL PAPER

**Yasuo Hachiya · Masaharu Hayashi
Satoko Kumada · Akira Uchiyama · Kuniaki Tsuchiya
Kiyoko Kurata**

Mechanisms of neurodegeneration in neuronal ceroid-lipofuscinoses

Received: 28 April 2005 / Revised: 10 November 2005 / Accepted: 10 November 2005 / Published online: 8 February 2006

Abstract Neuronal ceroid-lipofuscinoses (NCL) are a group of neurodegenerative diseases and autosomal recessive lysosomal storage disorders. We examined the involvement of cell death, oxidative stress, and glutamate excitotoxicity using immunohistochemistry against Bcl-2, Bcl-x, oxidative products to proteins, lipids and DNA, calcium-binding proteins (calbindin-D28K, parvalbumin, calretinin), and glial glutamate transporters (excitatory amino acid transporters 1 and 2), in addition to terminal deoxynucleotidyl transferase-mediated dUTP-nick end labeling (TUNEL) in the brains from three cases of late infantile form of NCL (LINCL) and one case of juvenile form of NCL (JNCL) to investigate the neurodegenerative mechanisms. In the cerebral and cerebellar cortex, all of three LINCL cases demonstrated neurons with TUNEL-immunoreactive nuclei, whereas the JNCL case did not show TUNEL-immunoreactive nuclei. The coexistence of the nuclear TUNEL-immunoreactivity nuclei and cytoplasmic deposition of 4-hydroxy-2-nonenal-modified protein in the frontal cortex and hypoglossal nucleus may suggest a possible interrelationship between DNA fragmentation and lipid oxidation in LINCL. Additionally, glycoxidation of protein and oxidative stress to DNA seemed to be involved in the cerebellar and cerebral degeneration, respectively. Interneurons immunoreactive for calbindin-D28K and parvalbumin were severely reduced in the cerebral cortex, whereas those for calretinin were comparatively well preserved in LINCL, indicating the possibility of altered GABAergic system. The disturbance of expression of glial glutamate transporters seemed to be heterogeneous and mild. These findings suggest the possibility of new treatments for neurodegeneration in LINCL using antioxidative agents and/or GABAergic medications.

Keywords Neuronal ceroid-lipofuscinosis · TUNEL · Immunohistochemistry · Oxidative stress · Calcium-binding proteins

Y. Hachiya (✉) · A. Uchiyama · K. Kurata
Department of Pediatrics, Metropolitan Fuchu Medical Center for SMID, 2-9-2 Musashi-dai, Fuchu-shi, 183-0042 Tokyo, Japan
E-mail: Yasuo_Hachiya@member.metro.tokyo.jp
Tel.: +81-42-3235115
Fax: +81-42-3226207

M. Hayashi
Department of Clinical Neuropathology, Tokyo Metropolitan Institute for Neuroscience, Tokyo, Japan

S. Kumada
Department of Neuropediatrics, Tokyo Metropolitan Neurological Hospital, Tokyo, Japan

K. Tsuchiya
Department of Laboratory Medicine, Tokyo Metropolitan Matsuzawa Hospital, Tokyo, Japan

Introduction

The neuronal ceroid-lipofuscinosis (NCL) is a group of fatal neurodegenerative diseases and autosomal recessive lysosomal storage disorders. The clinical presentation is composed of progressive motor and mental deterioration, visual loss, and uncontrolled epilepsy. The histological findings of NCL are characterized by accumulation of autofluorescent storage materials in neurons and many types of cells. Most forms of NCL show an autosomal recessive trait and their incidence is about 1 in 20,000. Until recently, the traditional subclassification of NCL was performed on the basis of the age of onset and the storage material at the ultrastructural level. Formerly, there had been the four main forms, i.e., infantile, classical late infantile (LINCL), juvenile (JNCL), and adult forms. However, due to the recent advances of molecular genetic and biochemical analysis, it is considered that the NCL is classified into eight genetic forms (CLN1-8) on the basis of the defect in six human genes responsible for the generation of human NCL [5, 6, 24, 28].

Late infantile NCL is caused by the mutations in the *CLN2* encoding tripeptidyl-peptidase1 (TPP1) [29] located on chromosome 11q15 [24, 28]. The symptoms of disease occur between 2 and 4 years, and consist of uncontrolled epilepsy, cognitive decline, ataxia, myoclonus, and blindness. Patients tend to show progressive myoclonic epilepsy, become bedridden during childhood, and die around the age of 20. The storage materials are immunoreactive for subunit c of the mitochondrial ATP synthase, and frequently demonstrate so-called curvilinear profiles on electron microscopy [18]. The JNCL is caused by the mutations in the *CLN3* encoding CLN3 protein that is located on chromosome 16p12 [24, 31]. The first symptom is onset of progressive visual failure between 4 and 7 years. Seizures appear in most patients between 7 and 18 years of age. The JNCL storage materials are also immunoreactive for subunit c of the mitochondrial ATP synthase, but consist of fingerprint bodies on electron microscopy [18]. Several CLN genes have been suggested to be critical for neuronal survival [4], but the mechanisms of neurodegeneration in addition to the relationships between clinical features and neuropathological findings have not been fully investigated in NCL [23]. Although epileptic seizures are frequently untreatable in LINCL and JNCL, epileptogenesis still remains to be clarified, and effective treatments have not been established for NCL.

In order to explore the neurodegenerative mechanisms in NCL, we immunohistochemically examined the involvement of apoptotic neuronal death, oxidative stress, and glutamate excitotoxicity in the brains from three LINCL cases and one JNCL case.

Materials and methods

Subjects

The clinical subjects comprised four cases of clinicopathologically confirmed NCL, and four age-matched controls without any pathological changes in the central nervous system aged 9–29 years (Table 1). Cases 1–3 suffered from LINCL, whereas only case 4 had JNCL. Cases 2 and 3 were siblings and their detailed neuropathological features were already reported [17]. Both LINCL cases and JNCL case showed mild to moderate depositions of lipopigment in the remaining neurons throughout the central nervous system regardless of neuronal loss (data not shown). The parent or family of each subject gave the consent to the neuropathological analysis. The brains were fixed in a buffered formalin solution for 2 weeks. The formalin-fixed brain was cut coronally, embedded in paraffin, and then subjected to hematoxylin and eosin, Klüver-Barrera, Bodian, and Holzer stainings. The NCL cases neuropathologically demonstrated various degrees of autofluorescent material deposition, neuronal loss, and gliosis (Table 1).

Table 1 Summary of clinico-pathological features of the NCL cases and controls

No.	Age (year) /sex	Disease form	Disease duration (year)	Myoclonic epilepsy	Onset of seizure (year)	Retinal degeneration	Postmortem time (h)	Brain weight (g)	Cerebral cortex	Hippocampus	Neuronal loss and gliosis		Cerebellar cortex	Medulla oblongata
											Striatum	Thalamus		
NCL cases														
1	8/Male	Late infantile	5	2+	5	1+	6	ND	1+	1+	1+	1+	1+	(−)
2	10/Male	Late infantile	7	2+	3	1+	4	445	2+	2+	2+	1+	2+	1+
3	12/Male	Late infantile	9	2+	3	1+	4	630	3+	2+	2+	2+	3+	2+
4	22/Male	Juvenile	11	1+	11	1+	2	800	1+	(−)	1+	1+	1+	(−)
No.	Age (year) /sex	Cause of death	Disease duration (year)	Myoclonic epilepsy	Onset of seizure (year)	Retinal degeneration	Postmortem time (h)	Brain weight (g)						
Controls														
1	9/Male	Leukemia	(−)	(−)	ND	(−)	4	ND						
2	16/Male	Myopathy	(−)	(−)	ND	(−)	6	1,505						
3	20/Male	Malignant hyperthermia	(−)	(−)	ND	(−)	3	ND						
4	29/Female	Guillain-Barre syndrome	(−)	(−)	ND	(−)	4	ND						

The degrees of lesions in routine histochemistry were graded by two independent observers (YH, MH) as (−), absent, 1+, mild and 2+, severe
h hour, *ND* not determined

Immunohistochemistry

Six-μm-thick sections were serially cut in selected brain regions including the frontal cortex, hippocampus, striatum, thalamus, cerebellum, and medulla oblongata. They were deparaffinized, quenched with 1% hydrogen peroxide, and treated after microwave antigen retrieval with the following antibodies: mouse monoclonal antibodies to advanced glycation end product (AGE) (Trans Genic Inc., Kumamoto, Japan), 4-hydroxynonenal (4-HNE), 8-hydroxy-2′-deoxyguanosine (8-OHdG) (Wako Pure Chemicals industries, Osaka, Japan), parvalbumin (Sigma-Aldrich, St Louis, MO, USA), Bcl-2, calbindin-D28K, calretinin, excitatory amino acid transporters 1 (EAAT1) and excitatory amino acid transporters 2 (EAAT2) (Novocastra Laboratories, Newcastle upon Tyne, UK), and rabbit polyclonal antibodies to Bcl-x (Santa Cruz Biotechnology, CA, USA) at the following concentrations: 1:40 (Bcl-2, EAAT1, EAAT2), 1:100 (parvalbumin, calbindin-D28K, calretinin), 1:1,000 (Bcl-x), 1:2,000 (AGE, 4-HNE, 8-OHdG). Immunohistochemistry for three calcium-binding proteins was performed only in the sections of the frontal cortex and hippocampus. Antibody binding was visualized by means of the avidin–biotin–immunoperoxidase complex method (Nichirei, Tokyo, Japan) following the manufacturer's protocol. No staining was confirmed in sections in the absence of either antibody. To determine the species of nucleoside in immunohistochemistry for 8-OHdG, pretreatment of the sections with DNase (10 U/μl at 37°C for 1 h, Invitrogen, Carlsbad, CA, USA) and RNase (5 U/μl at 37°C for 1 h, Invitrogen, Carlsbad, CA, USA) was examined. Neuronal lipopigments were not immunoreactive for any of cell death-related proteins, oxidative products, calcium-binding proteins, and glutamate transporters.

Terminal deoxynucleotidyl transferase-mediated dUTP-nick end labeling (TUNEL)

Sections were treated after microwave antigen retrieval with monoclonal antibody against neurofilament at 1:50 dilution (DakoCytomation, Glostrup, Denmark) and 4-HNE (the aforementioned antibody and dilution) overnight. Antibody binding was visualized by means of the avidin–biotin–3-amino-9-ethyl-carbazole complex method (DakoCytomation, Glostrup, Denmark) following the manufacturer's protocol. After washing, sections were treated with 0.1% trypsin solution at 37°C for 30 min and incubated in Tris-buffered saline containing terminal deoxynucleotidyl transferase (0.3 U/μl) (Life Technologies, Gaithersburg, MD) and digoxigenin-labeled 2′-deoxyuridine 5′-triphosphate (0.01 nmol/μl, Roche Diagnostics GmbH, Mannheim, Germany) at 37°C for 60 min. Then, they were treated with a 1:500 dilution of alkaline phosphatase-labeled anti-digoxigenenin antibodies (Roche Diagnostics GmbH) at room temperature for 1 h. The reaction was visualized by 4-nitroblue-tetrazolium-chloride/5-bromide-4-chloride-3-indolyl-phosphate (Sigma-Aldrich, St Louis, MO, USA).

Quantitative analysis

The degree of immunoreactivities for oxidative products was graded by two independent observers (YH, MH) in controls and NCL cases as (−), absent, 1+, mildly deposited and 2+, severely deposited. The degree of reduced immunoreactivities for EAATs was graded by two independent observers (YH, MH) in comparison with that in controls as (−), not altered, 1−, mildly affected and 2−, severely affected. The number of neurons with TUNEL-immunoreactive nuclei in the frontal cortex, striatum, thalamus and cerebellar cortex, in addition to that of neurons immunoreactive for calcium-binding proteins in the frontal cortex, was counted to gain the density of immunoreactive neurons. Cell counts were performed following manual labeling of appropriate cells in ten microscopic subfields at 100× magnification using a counting box (0.25 mm^2), and each averaged density was expressed as the mean ± SD. On the other hand, the number of the whole immunoreactive neurons immunoreactive for calcium-binding proteins and TUNEL-immunoreactive nuclei was quantified in the hippocampus, subiculum, and/or the hypoglossal nucleus. Two neuropathologists (YH, MH) independently performed both the visual inspection of staining intensity and quantitative evaluation of the immunoreactive cells without knowledge of the diagnosis, and the inter-measurement coefficient of variation was under 5% in any quantitative analysis.

Results

Analysis of cell death

Four controls (data not shown) and case 4 of JNCL showed no TUNEL-immunoreactive nuclei in all the brain regions examined, although the hippocampus and hypoglossal nucleus were not investigated in case 4. All three cases of LINCL exhibited neurons with nuclei immunoreactive for TUNEL in the frontal cortex and cerebellar granule cells (Table 2). In the hippocampus, subiculum, and hypoglossal nucleus, cases 2 and 3 but not case 1 demonstrated neurons with nuclei immunoreactive for TUNEL (Fig. 1a, b). Only case 3 had a few nuclei immunoreactive for TUNEL in the striatum and thalamus. The whole number of the neurons with nuclei immunoreactive for TUNEL in cases 2 and 3 with long disease duration tended to be mildly higher than that in case 1. Immunohistochemistry for Bcl-2 failed to visualize immunoreactive structures in both the NCL cases and

Table 2 Summary of nuclei immunoreactive for TUNEL and immunohistochemistry for 4-HNE

No.	Frontal cortex	Hippocampus	Subiculum	Striatum/thalamus	Cerebellar cortex		Hypoglossal nucleus
					Granule cells	Purkinje cells	
Terminal deoxynucleotidyl transferase-mediated dUTP-nick end labeling							
1	8.6 ± 4.3	0	0	0	15.8 ± 2.69	0	0
2	162.2 ± 29.2	330	87	0	5.8 ± 1.30	0	9
3	101 ± 18.3	182	20	15.0 ± 4.36	126.8 ± 25.53	0	28
4	0	ND	ND	0	0	0	ND
Immunohistochemistry for 4-hydroxynonenal							
1	1+	1+	1+	(−)	(−)	2+	(−)
2	2+	(−)	(−)	(−)	(−)	1+	1+
3	2+	(−)	(−)	(−)	(−)	1+	1+
4	(−)	ND	ND	(−)	(−)	1+	ND

The number of neurons with TUNEL-immunoreactive nuclei was counted following manual labeling of appropriate cells in ten microscopic subfields at 100× magnification using a counting box (0.25 mm^2), and each averaged density was expressed as the mean ± SD. The degree of immunoreactivity for 4-HNE was graded by two independent observers (YH, MH) in comparison with that in controls as (−), absent, 1+, mild and 2+, severe. Controls did not demonstrate any TUNEL-immunoreactive nuclei or immunoreactivity for 4-HNE
ND not determined

controls, although the lymphoma cells in the lymph node from patients with malignant lymphoma were immunoreactive for Bcl-2 (data not shown). The perinuclear cytoplasm but not accumulated lipopigments in the remaining neurons and/or the neuropils was immunoreactive for Bcl-x in the frontal cortex, basal ganglia, Purkinje cells, and gray matter in the brainstem in both the LINCL cases and controls (Fig. 1c), whereas case 4 of JNCL showed a reduced immunoreactivity in the neuropils in the frontal cortex in addition to the Purkinje cells (Fig. 1d).

Analysis of oxidative damage

All four controls exhibited no immunoreactive structures for either of 4-HNE, AGE, or 8-OHdG. All NCL cases, and more predominantly the LINCL cases, demonstrated 4-HNE immunoreactivity in the perinuclear cytoplasm, but not in the accumulated lipopigments, in the remaining neurons located throughout the brain except in the striatum and thalamus (Fig. 2a, Table 2). It has been reported that 4-HNE can induce apoptosis [19], and there seemed to be the favorable occurrence of

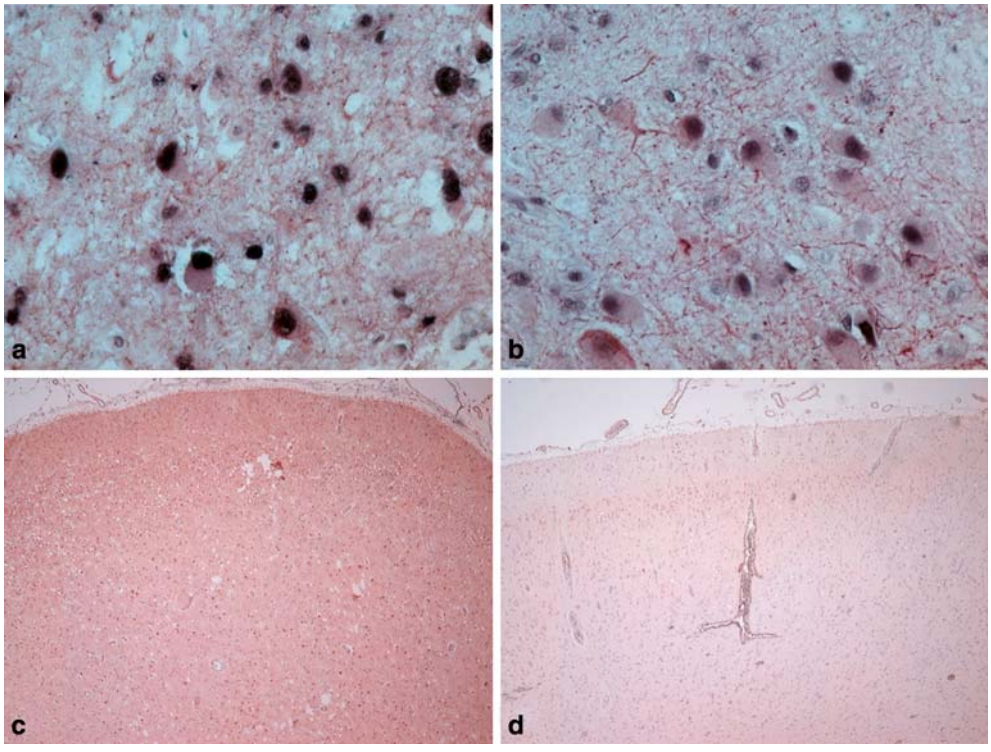

Fig. 1 Representative illustrations of analysis for cell death. Nuclei densely immunoreactive for TUNEL were observed in most of the neurons with swollen cytoplasm in the frontal cortex of case 3 (**a**) and the hippocampus of case 2 (**b**), 400×. The neuropil immunoreactivity for Bcl-x in the frontal cortex was comparatively well preserved in case 1 (**c**), whereas that was reduced in case 4 (**d**), 40×

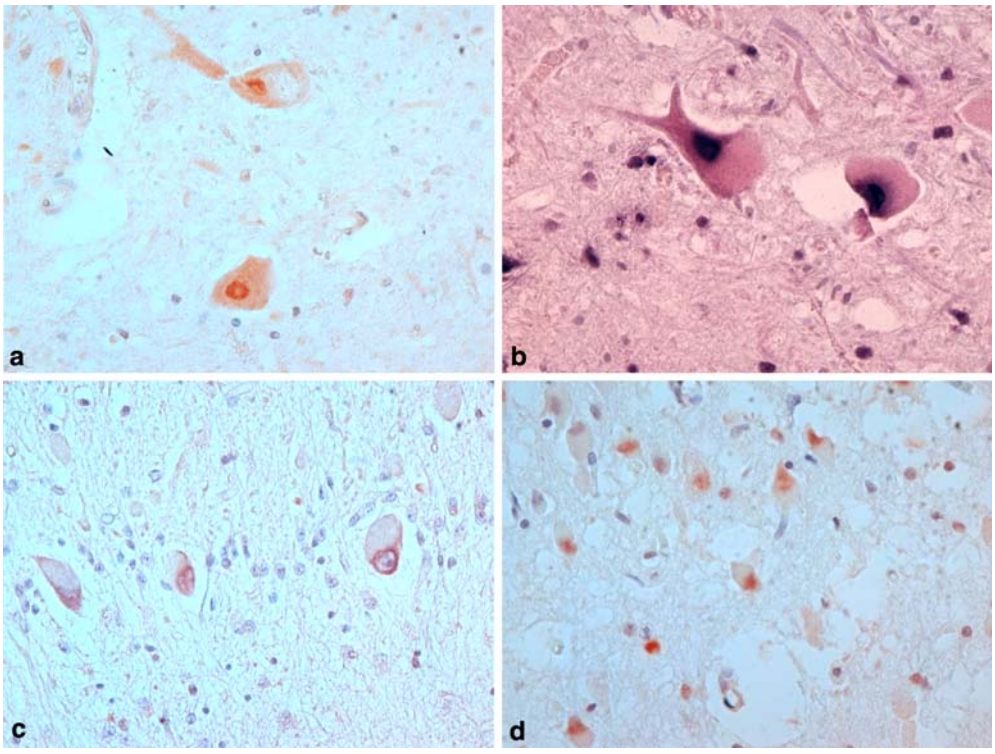

Fig. 2 Representative illustrations in analysis for oxidative damage. Perinuclear immunoreactivity for 4-HNE was found in the remaining hypoglossal neurons of case 2 (**a**), 400×. The nuclear TUNEL-immunoreactivity (*purple*) and perinuclear immunoreactivity for 4-HNE (*red*) coexisted in two neurons of the hypoglossal nucleus in case 3 (**b**), 400×. Case 1 showed perinuclear immunoreactivity for AGE in the remaining Purkinje cells (**c**, 400×), while case 4 had nuclear immunoreactivity for 8-OHdG in the remaining small pyramidal neurons with swollen cytoplasm of the frontal cortex (**d**, 400×)

TUNEL-immunoreactive nuclei and 4-HNE-immunoreactive neurons in the frontal cortex, cerebellar cortex, and hypoglossal nucleus in the LINCL cases (Table 2). In our study, TUNEL-positive nuclei and 4-HNE positive neurons were found in the same brain regions, such as the frontal cortex, cerebellar cortex, and hypoglossal nucleus in the LINCL cases (Table 2). The perinuclear cytoplasm of the remaining Purkinje cells was visualized by immunohistochemistry for AGE in three LINCL cases in addition to the neurons in the hypoglossal nuclei in case 3 (Fig. 2c, Table 3). In contrast, case 4 of JNCL did not show any immunoreactive structures for AGE. The nuclei immunoreactive for 8-OHdG were found in the frontal cortex in all four NCL cases, and it was also observed in one or two of the LINCL cases in the striatum, thalamus, cerebellar granule cells, and hypoglossal nucleus (Fig. 2d, Table 3). Nuclear immunoreactivity for 8-OHdG was attenuated by pretreatment with DNase but not RNase (data not shown).

Expressions of calcium-binding proteins and glial glutamate transporters

In the frontal cortex in controls, the interneurons immunoreactive for calbindin-D28K and parvalbumin were identified in the second and third layers and predominantly in the fourth layers, respectively, while those for calretinin were more diffusely scattered from the second layer to the fifth one (Fig. 3). In the NCL cases, interneurons immunoreactive for calbindin-D28K and parvalbumin were severely reduced (Table 4, Fig. 3). On

Table 3 Summary of immunohistochemistry for oxidative products

No.	Immunoreactivity for advanced glycation end product	Immunoreactivity for 8-hydroxy-2′-deoxyguanosine				
		Frontal cortex	Hippocampus	Striatum/thalamus	Cerebellar granule cells	Hypoglossal nucleus
1	Purkinje cells 2+	1+	(−)	1+	(−)	(−)
2	Purkinje cells 1+	1+	(−)	1+	(−)	1+
3	Purkinje cells 1+ Hypoglossal nucleus 1+	2+	(−)	(−)	2+	2+
4	(−)	1+	(−)	(−)	(−)	(−)

The degree of immunoreactivities for oxidative products was graded by two independent observers (YH, MH) in controls and NCL cases as (−), absent, 1+, mildly deposited and 2+, severely deposited. Controls did not demonstrate any immunoreactivity for either oxidative product

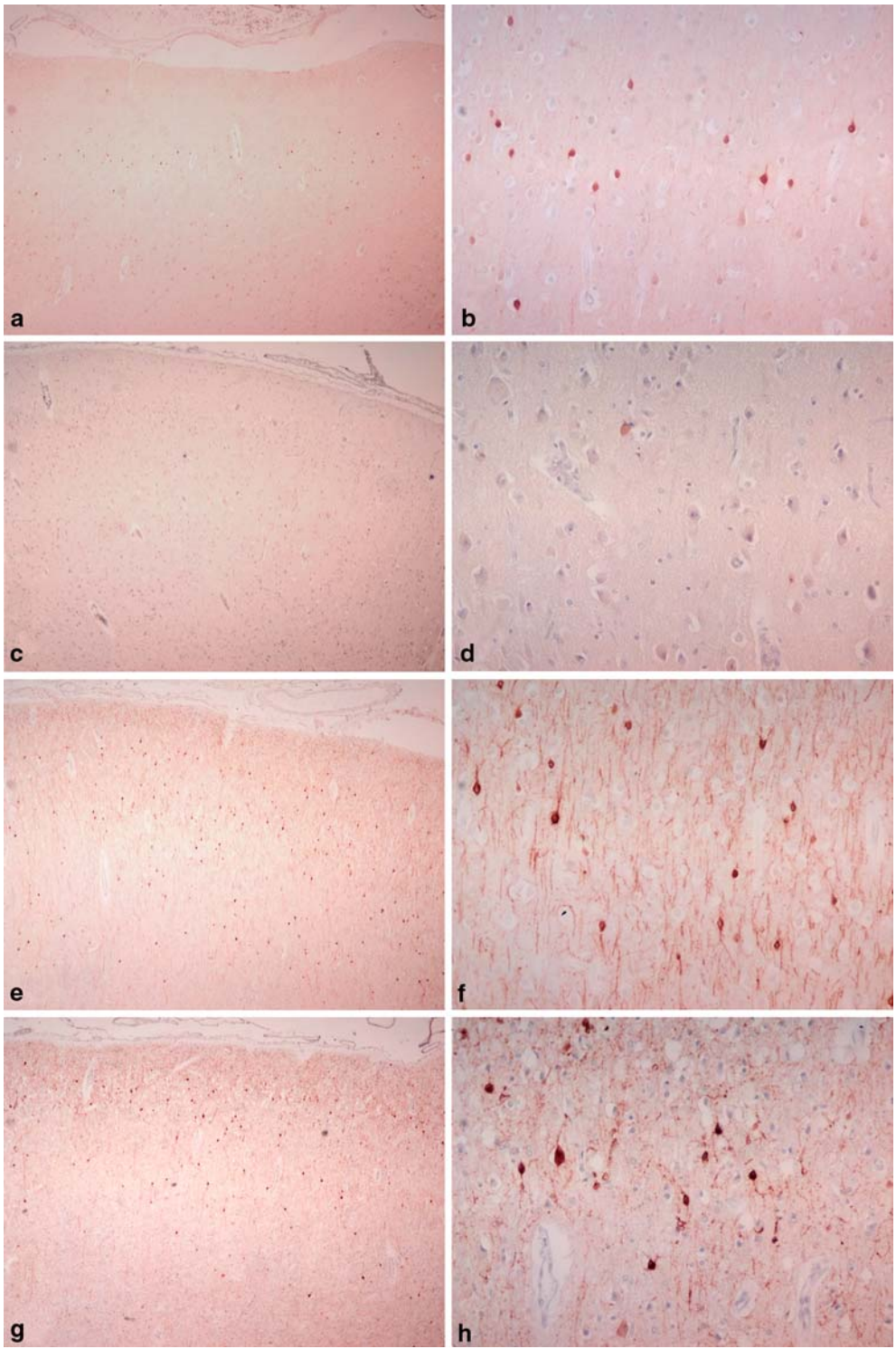

Fig. 3 Representative illustrations on expression of calcium-binding proteins. Interneurons immunoreactive for calbindin-D28K (**a**–**d**) were scattered around the second layer in the frontal cortex of control 1 (**a** 40×; **b** 200×) and LINCL case 1 (**c** 20×; **d** 200×). Interneurons immunoreactive for calretinin were comparatively well preserved in the frontal cortex of both control 1 (**e** 40×; **f** 200×) and case 1 (**g** 40×; **h** 200×)

the other hand, interneurons immunoreactive for calretinin were comparatively well preserved in the hippocampus and subiculum in all NCL cases in addition to the frontal cortex in case 4, whereas they mildly to moderately decreased in inverse proportion to the disease duration in the frontal cortex in the LINCL cases (Table 4). Additionally, interneurons immunoreactive for calretinin were also well preserved in the frontal cortex (Table 4, Fig. 3).

In controls, the neuropil of the frontal cortex, hippocampus, striatum, thalamus, cerebellar molecular layer, and gray matter in the brainstem was immuno-

Table 4 Summary of interneurons immunoreactive for calcium-binding proteins in the cerebral cortex

No.	Frontal cortex			Hippocampus			Subiculum		
	Calbindin -D28K	Parvalbumin	Calretinin	Calbindin-D28K	Parvalbumin	Calretinin	Calbindin -D28K	Parvalbumin	Calretinin
NCL cases									
1	1.3 ± 1.5	0.3 ± 0.6	24.7 ± 8.8	2	0	86	1	0	125
2	1.7 ± 1.2	0.6 ± 0.5	11.9 ± 4.6	3	0	52	0	0	57
3	0.3 ± 0.5	1.2 ± 2.4	7.9 ± 1.8	1	1	108	0	0	57
4	0.5 ± 0.9	3.5 ± 3.3	51 ± 15.5	4	1	111	2	0	87
Mean ± SD	1.0 ± 0.7	1.4 ± 1.5	23.8 ± 19.5	2.5 ± 1.3	0.5 ± 0.6	89.3 ± 27.2	0.8 ± 1.0	0	81.5 ± 32.3
Controls									
1	7.5 ± 2.2	25.6 ± 3.5	32.5 ± 4.1	23	5	81	22	19	62
2	5.4 ± 1.2	24.8 ± 3.5	34.1 ± 3.1	37	22	82	36	36	79
3	13.9 ± 1.9	17.4 ± 2	26.9 ± 2.4	66	ND	89	43	ND	55
4	7.7 ± 0.9	16.7 ± 2	26.6 ± 2.7	45	26	92	35	49	62
Mean ± SD	8.6 ± 3.7	21.1 ± 4.7	42.8 ± 3.8	42.8 ± 18.0	17.7 ± 11.2	86 ± 5.4	34 ± 8.8	34.7 ± 15.0	64.5 ± 10.2

The number of interneurons immunoreactive for calcium-binding proteins was counted following manual labeling of appropriate cells in ten microscopic subfields at 100× magnification using a counting box (0.25 mm^2), and each averaged density was expressed as the mean ± SD

ND not determined

reactive for EAAT1 and EAAT2 (Fig. 4a, c). Reduced immunoreactivity for both glial glutamate transporters was noticed in the various brain regions in cases 2 and 3, while that was recognized only in the cerebellar molecular layer in case 1 (Table 5, Fig. 4b, d). And the brain regions showing reduced EAAT1 expressions were more extended than those showing EAAT2 expressions in cases 2 and 3. In contrast, case 4 of JNCL demonstrated well-preserved immunohistochemistry for EAAT1, and reduced immunohistochemistry for EAAT2 localized in the thalamus and medulla oblongata (Table 5).

Discussion

TUNEL is a useful method to detect DNA fragmentation in pathological tissues, although it cannot distinguish apoptosis and necrosis especially in autopsy specimens, and long postmortem time may affect the TUNEL reac-

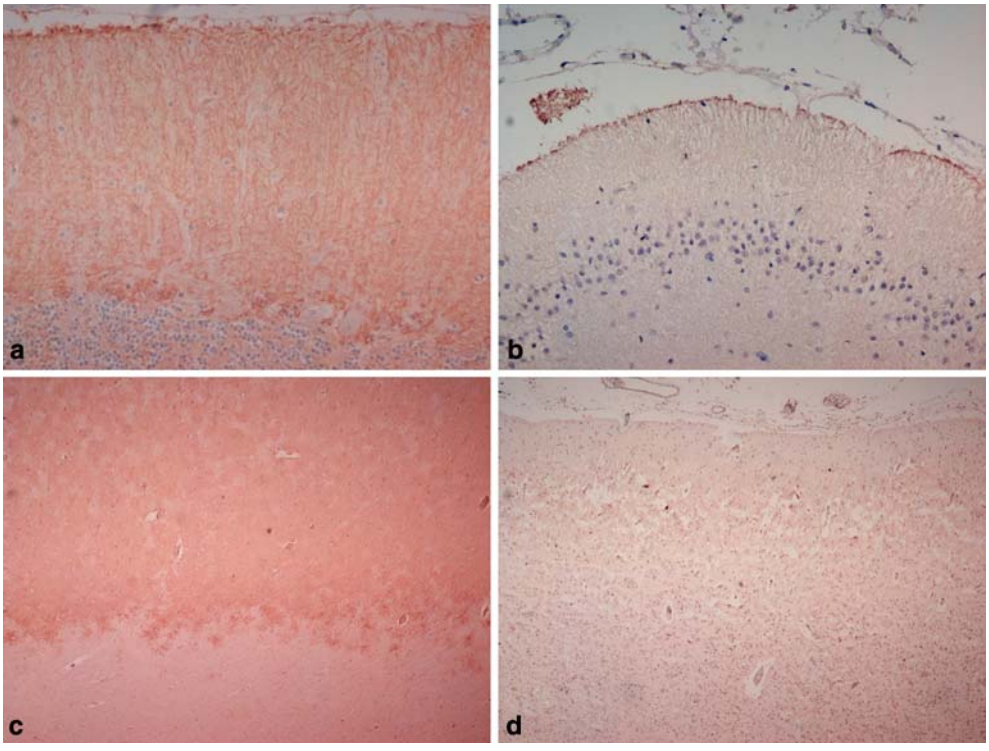

Fig. 4 Representative illustrations on expression of glial transporters. Immunoreactivities for EAAT1 were observed in the fine fibers of the molecular layer in control 3 (**a** 200×) but not in LINCL case 3 (**b** 200×). Neuropil immunoreactivities for EAAT2 were visualized in the frontal cortex in control 1 (**c** 40×) but not in case 3 (**d** 20×). The upper two-third of the illustrations demonstrated the cerebral cortex in **c** and **d**

Table 5 Summary of immunohistochemistry for glial glutamate transporters

No.	Reduced immunoreactivity for excitatory amino acid transporter 1					Reduced immunoreactivity for excitatory amino acid transporter 2				
	Frontal cortex	Hippocampus	Striatum /thalamus	Cerebellar molecular layer	Medulla oblongata	Frontal cortex	Hippocampus	Striatum /thalamus	Cerebellar molecular layer	Medulla oblongata
1	(−)	(−)	(−)	1−	(−)	(−)	(−)	(−)	1−	(−)
2	1−	1−	1−	1−	1−	(−)	(−)	1−	1−	(−)
3	1−	1−	1−	2−	1−	1−	(−)	1−	2−	(−)
4	(−)	(−)	(−)	(−)	(−)	(−)	(−)	1−	(−)	1−

The degree of immunoreactivities for glial glutamate transporters was graded by two independent observers (YH, MH) in comparison with that in controls as (−), absent, 1−, mild and 2−, severe

tivity [8, 16]. In this analysis, cases 2 and 3 of LINCL showed neurons with TUNEL-immunoreactive nuclei in the cerebral and cerebellar cortex in addition to the hypoglossal nucleus. Since the severe neuronal loss may affect the number of neurons with TUNEL-immunoreactive nuclei in cases 2 and 3 (Tables 1, 2), the longer disease duration is speculated to generate more TUNEL-immunoreactive neurons in LINCL in those cases than case 1. Both cases had postmortem time shorter than 5 h, but the remaining neurons in the cases did not show altered expressions of cell death-related proteins including Bcl-2 family proteins. Accordingly, it is not definite that TUNEL immunoreactivity can be evidence of apoptotic neuronal death in the brains of LINCL. On the other hand, case 4 of JNCL showed change in the Bcl-x expression in the cerebral and cerebellar cortices, although there was no TUNEL immunoreactivity in the brain regions examined, and the antibody used in this analysis cannot discriminate the longer protein Bcl-xL blocking cell death from the shorter protein Bcl-xS facilitating cell death [16]. Although several research groups have pointed out the involvement of apoptotic neuronal death in LINCL and JNCL [5, 19, 23, 27], the involvement of apoptosis in LINCL and JNCL should be examined in extended number of cases.

4-hydroxynonenal protein is one of the major products of membrane lipid oxidation which is well known to be a toxic product in oxidative damage [32]. The increasing expression of 4-HNE has been demonstrated in the brains in both adult-onset neurodegenerative disorders such as Alzheimer's and Parkinson's diseases [14, 35], and child-onset ones such as hereditary nucleotide repair disorders, subacute sclerosing panencephalitis, and spinal muscular atrophy [9–11]. Similarly in the NCL cases, the immunoreactivity for 4-HNE in the perinuclear cytoplasm of the remaining neurons was observed in widespread brain regions. The perinuclear localization can be caused by accumulated lipopigments in the cytoplasm, because lipopigments, not being immunoreactive for either oxidative product, occupied most of the cytoplasm in the remaining neurons. There has been a report that 4-HNE can induce apoptosis with activation of caspases leading to DNA fragmentation [20]. Also in this analysis, the LINCL cases 2 and 3 demonstrated co-localization of the nuclear TUNEL-immunoreactivity and cytoplasmic deposition of 4-HNE (Table 2, Fig. 2b) in the frontal cortex and hypoglossal nucleus. Furthermore, case 1 showed cytoplasmic deposition of 4-HNE in the hippocampus and subiculum, although the case lacked the nuclear TUNEL-immunoreactivity in the same brain regions. In the cerebellar cortex of three LINCL cases, the nuclear TUNEL-immunoreactivity and cytoplasmic deposition of 4-HNE were found in the granule cells and Purkinje cells, separately. Taken together, the interrelationship between DNA fragmentation and lipid oxidation may be complex and different between the brain regions, and that still remains to be elucidated. The AGE is considered as a marker of protein damage by glycoxidation, and shows an abnormal deposition in the various aforementioned neurodegenerative disorders [15, 30]. The immunoreactivity for AGE was found in the Purkinje cells in all LINCL cases and in the neurons in the hypoglossal nuclei in case 3, but not in JNCL case. Herein the protein glycoxidation can be involved in the cerebellar degeneration more predominantly in LINCL than JNCL. Oxidative damage to DNA can induce the 8-OHdG, which has been one of the most popular markers for evaluation of oxidative stress to nucleosides. Nunomura et al. suggested an association between oxidative damage to nucleosides and deposition of amyloid-β in Alzheimer's disease [3, 25]. In the previous studies, we clarified the increased occurrence of 8-OHdG-immunoreactive nuclei in the cerebral cortex at acute stage in subacute sclerosing panencephalitis, the brain regions involved in motor control except for the motor neurons in spinal muscular atrophy, and the globus pallidus in the xeroderma pigmentosum group A [10, 12, 13]. Both the LINCL and JNCL cases had the nuclear immunoreactivity for 8-OHdG in the frontal cortex in common, whereas each NCL case additionally showed it in the various brain regions. It is likely that oxidative damage to DNA might be related to the neurodegeneration of the cerebral cortex. Although oxidative stress has rarely been examined in progressive myoclonic epilepsy [2], this analysis strongly indicated the possibility

of its involvement in the neurodegeneration of LINCL, and JNCL requires further investigation.

Calcium-binding proteins, including calbindin-D28K, parvalbumin, and calretinin, regulate intracellular calcium concentrations in the neurons through their buffering capacity and selectively identify the populations of GABAergic interneurons [7]. In the cerebral cortex of the controls, the interneurons immunoreactive for each calcium-binding protein demonstrated the layer-specific and regional distribution pattern (Fig. 3). This analysis showed that the expressions of calcium-binding proteins were altered in the cerebral cortex, hippocampus, and subiculum in both the LINCL and JNCL cases (Table 4), indicating the possible disturbance of the GABAergic interneurons in the cerebral cortical degeneration in NCL. Interneurons immunoreactive for both calbindin-D28K and parvalbumin were severely reduced in all the brain regions examined. In contrast, those for calretinin seemed to be spared in the hippocampus and subiculum in all the NCL cases and in the frontal cortex in JNCL case 4, although that was affected in the LINCL cases with longer survival. Recently, Tyynelä et al. [33] clarified the loss of interneurons in the hippocampus in several forms of NCL including LINCL using immunochemistry for calcium-binding proteins, although that study only had one LINCL case, and the other cerebral cortices were not examined. Additionally, the reduction of the GABAergic interneurons labeled with glutamic acid decarboxylase has been reported in the brains of animal models of lysosomal storage disorders [34]. It is intriguing that the similar selective reductions of calbindin-D28K- and parvalbumin-immunoreactive interneurons were reported in the entorhinal cortex in Alzheimer's disease [22] and in the prefrontal cortex in schizophrenia [1]. These data suggest that the calretinin-immunoreactive interneurons may be more resistant to neurodegeneration irrespective of the type of disorders. Glial glutamate transporters modulate neurotransmission by maintaining low concentrations of extracellular glutamate and prevent glutamate excitotoxicity [7]. The constitutive expressions of the EAAT1 and EAAT2 by astrocytes were well visualized in the neuropil of the gray matter in controls (Fig. 3) and disturbed expression of glutamate transporters is well established in temporal lobe epilepsy [2, 21, 26]. In LINCL, reduced immunoreactivities for both glial transporters were observed predominantly in the sibling cases 2 and 3, whereas case 1 with shorter survival only showed those in the cerebellar cortex. The length of disease duration might cause the differences among the three LINCL cases, but the changes of expressions of EAAT seemed to be milder and more heterogeneous than the aforementioned altered expressions of calcium-binding proteins in the cerebral cortex.

As a conclusion, various oxidative products were accumulated in the brain in LINCL, and it is likely that oxidative stress may have a more important role in neurodegeneration than apoptotic DNA fragmentation, although lipid peroxidation might be related to DNA fragmentation. In terms of the balance between the inhibitory and excitatory neuron systems, the disturbance of inhibitory GABAergic interneurons was superior to glutamate excitotoxicity in the degeneration of the cerebral cortex. Since we mainly focused on cases of LINCL in this analysis, the extended study in cases of other forms including JNCL is necessary for the further investigation of pathomechanisms in NCL. However, immunohistochemical findings in this analysis suggest the possibility of new treatments for neurodegeneration in LINCL using antioxidative agents and/or GABAergic medications. And we strongly believe that the immunohistochemical examination in autopsy brains will give us a clue to the development of new treatments.

References

1. Beasley CL, Zhang ZJ, Patten I, Reynolds GP (2002) Selective deficits in prefrontal cortical GABAergic neurons in schizophrenia defined by the presence of calcium-binding proteins. Soc Biol Psychiatry 52:708–715
2. Ben-Manachem E, Kyllerman M, Marklund S (2000) Superoxide dismutase and glutathione peroxidase function in progressive myoclonus epilepsies. Epilepsy Res 40:33–39
3. Emerit J, Edeas M, Bricarie F (2004) Neurodegenerative diseases and oxidative stress. Biomed Phamacother 58:39–46
4. Ezaki J, Kominami E (2004) The intracellular location and function of proteins of neuronal ceroid lipofuscinoses. Brain Pathol 14:77–85
5. Goebel HH, Wisniewski KE (2004) Current state of clinical and morphological features in human NCL. Brain Pathol 14:61–69
6. Haltia M (2003) The neuronal ceroid-lipofuscinoses. J Neuropathol Exp Neurol 62:1–13
7. Hayashi M (2001) Neuropathology of the limbic system and brainstem in West syndrome. Brain Dev 23:516–522
8. Hayashi M, Arai N, Murakami T, Morimatsu Y, Oda M, Matsuyama H (1998) A study of cell death in Werdnig Hoffmann disease brain. Neurosci Lett 243:117–120
9. Hayashi M, Itoh M, Araki S, Kumada S, Shioda K, Tamagawa K, Mizutani T, Morimatsu Y, Minagwa M, Oda M (2001) Oxidative stress and glutamate transport in hereditary nucleotide repair disorders. J Neuropathol Exp Neurol 60:350–356
10. Hayashi M, Arai N, Satoh J, Suzuki H, Katayama K, Tamagawa K, Morimatsu Y (2002) Neurodegenerative mechanisms in subacute sclerosing panencephalitis. J Child Neurol 17:725–730
11. Hayashi M, Araki S, Arai N, Kumada S, Itoh M, Tamagawa K, Oda M, Morimatsu Y (2002) Oxidative stress and disturbed glutamate transport in spinal muscular atrophy. Brain Dev 24:770–775
12. Hayashi M, Araki S, Kohyama J, Shioda K, Futamatsu R, Tamagawa K (2004) Brainstem and basal ganglia lesions in xeroderma pigmentosum group A. J Neuropathol Exp Neurol 63:1048–1057
13. Hayashi M, Araki S, Kohyama J, Shioda K, Fukatsu R (2005) Oxidative nucleotide damage and superoxide dismutase expression in the brains of xeroderma pigmentosum group A and Cockayne syndrome. Brain Dev 27:34–38
14. Jenner P (2003) Oxidative stress in Parkinson's disease. Ann Neurol 53:S26–S38
15. Kikuchi S, Shinpo K, Takeuchi M, Yamagishi S, Makita Z, Sasaki N, Tashiro K (2003) Glycation—a sweet tempter for neuronal death. Brain Res Brain Res Rev 41:306–323
16. Kumada S, Hayashi M, Mizuguchi M, Nakano I, Morimatsu Y, Oda M (2000) Cerebellar degeneration in hereditary dentatorubral-pallidoluysian atrophy and Machado–Joseph disease. Acta Neuropathol 99:48–54

17. Kurata K, Hayashi M, Satoh J, Kojima H, Nagata J, Tamagawa K, Shinohara T, Morimatsu Y, Kominami E (1999) Pathological study on sibling autopsy cases of the late infantile form of neuronal ceroid lipofuscinosis. Brain Dev 21:63–67
18. Lake BD, Hall NA (1993) Immunolocalization studies of subunit c in late infantile and juvenile Batten disease. J Inherit Metab Dis 16:263–266
19. Lane SC, Jolly RD, Schmechel DE, Alroy J, Boustany RM (1996) Apoptosis as the mechanism of neurodegeneration in Batten's disease. J Neurochem 67:677–683
20. Liu W, Kato M, Akhand AA, Hayakawa A, Suzuki H, Miyata T, Kurokawa K, Hotta Y, Ishikawa N, Nakashima I (2000) 4-hydroxynonenal induces a cellar redox status-related activation of the caspase cascade for apoptotic cell death. J Cell Sci 113:635–641
21. Mathern GW, Mendoza BS, Lozada BS, Pretorius JK, Dehnes Y, Danbolt NC, Nelson N, Leite JP, Chimelli L, Born DE, Sakamoto AC, Assirati JA, Fried I, Peacock WJ, Ojemann GA, Adelson PD (1999) Hippocampal GABA and glutamate transporter immunoreactivity in patients with temporal lobe epilepsy. Neurology 52:453–472
22. Mikkonen M, Alafuzoff I, Tapiola T, Soininen H, Miettinen R (1999) Subfield- and layer-specific changes in parvalbumin, calretinin and calbindin-D28 immunoreactivity in the entorhinal cortex in Alzheimer's disease. Neuroscience 92:515–532
23. Mitchison HM, Lim MJ, Cooper JD (2004) Selectivity and types of cell death in the neuronal ceroid lipofuscinoses. Brain Pathol 14:86–96
24. Mole SE (2004) The genetic spectrum of human neuronal ceroid-lipofuscinoses. Brain Pathol 14:70–76
25. Nunomura A, Perry G, Aliev G, Hirai K, Takeda A, Balraj EK, Jones PK, Ghanbari H, Wataya T, Shimohama S, Chiba S, Atwood CS, Petersen RB, Smith MA (2001) Oxidative damage is the earliest event in Alzheimer disease. J Neuropathol Exp Neurol 60:759–767
26. Proper EA, Hoogland G, Kappen SM, Jansen GH, Rensen MG, Schrama LH, van Veelen CW, van Rijen PC, van Nieuwenhuizen O, Gispen WH, de Graan PN (2002) Distribution of glutamate transporters in the hippocampus of patients with pharmaco-resistant temporal lobe epilepsy. Brain 125:32–43
27. Puranam KL, Guo WX, Qian WH, Nikbakht K, Boustany RM (1999) CLN3 defines a novel antiapoptotic pathway operative in neurodegeneration and mediated by ceramide. Mol Genet Metab 66:294–308
28. Sharp JD, Wheeler RB, Lake BD, Savukoski M, Jarvela IE, Peltonen L, Gardiner RM, Williams RE (1997) Loci for classical and a variant late infantile neuronal ceroid lipofuscinoses map to chromosomes 11p15 and 15q21–23. Hum Mol Genet 6:591–595
29. Sleat DE, Donnelly RJ, Lackland H, Liu CG, Sohar I, Pullarkat RK, Lobel P (1997) Association of mutations in a lysosomal protein with classical late-infantile neuronal ceroid-lipofuscinosis. Science 277:1802–1805
30. Takedo A, Yasuda T, Miyata T, Mizuno K, Li M, Yoneyama S, Horie K, Maeda K, Sobue G (1996) Immunohistochemical study of advanced glycation end products in aging and Alzheimer's disease brain. Neurosci Lett 221:17–20
31. The International Batten Disease Consortium (1995) Isolation of a novel gene underlying Batten disease, CLN3. Cell 82:949–957
32. Toyokuni S (1999) Reactive oxygen species-induced molecular damage and its application in pathology. Pathol Int 49:91–102
33. Tyynelä J, Cooper JD, Khan MN, Shemilts SJ, Haltia M (2004) Hippocampal pathology in the human neuronal ceroid-lipofuscinoses: distinct patterns of storage deposition, neurodegeneration and glial activation. Brain Pathol 14:349–357
34. Walkley SU (1998) Cellular pathology of the lysosomal strage disorders. Brain Pathol 8:175–193
35. Zarkovic K (2003) 4-hydroxynonenal and neurodegenerative diseases. Mol Aspects Med 24:293–303